JOURNAL OF AIRCRAFT
Vol. 32, No. 3, May–June 1995

Prediction of Airplane States

Amnon Katz* and Kenneth Graham†
University of Alabama, Tuscaloosa, Alabama 35487-0280

Methods for extrapolation of airplane flight trajectory and orientation history that exploit coordinated flight and other airplane specific grounds are derived and applied. They include extraction of orientation from trajectory with angle-of-attack (AOA) correction, closed-form trajectory extrapolation based on constant longitudinal and transverse acceleration, and a "phugoid scheme" for six degrees-of-freedom extrapolation at constant AOA in coordinated flight. A metric well known in connection with networked simulation shows an advantage of up to a factor of 3 for the new methods.

I. Introduction

THE state of a rigid body in three-space involves six degrees of freedom (DOF). The motion history of such body is defined by six arbitrary functions. Current extrapolation schemes are based on the assumption that these six functions are smooth. Airplane dynamics admits only four arbitrary functions, and for most practical purposes only three. We exploit this knowledge for improved prediction for airplanes.

This work originated in the context of distributed interactive simulation (DIS) and the DIS standard.[1] The standard exploits the extrapolation of the motion of simulated entities to reduce data transmissions over the network. An update is broadcast only when the extrapolation breaks a preselected tolerance. In this way, a natural metric for the fidelity of the extrapolation arises: the frequency of required updates becomes the measure of fidelity. The better the prediction of future motion, the less frequent the updates.

We compare the new methods, in terms of frequency of required updates, to second-order prediction of position and first-order prediction of orientation (based on constant angular velocity).[2] We also compare our results to the use of perfect position or of perfect orientation. Our methods provide an improvement by a factor of 2 to 3 over the generic comparison method. Extracted orientation often rates close to perfect orientation.

II. Overview

Extrapolation in time is prediction. Naturally, it is impossible to predict what a pilot will do. But a pilot does not control six arbitrary functions, he (the word "he" in all its forms is used here generically to mean he, she, or it) controls only four in the form of his inputs to the throttle, elevator, ailerons, and rudder. If the added assumption is made that coordinated flight be maintained, then only three DOF remain. Coordinated flight will be assumed from here on.

Three arbitrary functions are exactly what is required to define a space–time trajectory. (A space–time trajectory is the combination of a curve in space and a schedule of the times at which the airplane is at any given point.) An airplane can (subject to some performance limitations) fly an arbitrarily specified smooth space–time trajectory; but its orientation while doing so is totally determined.

To visualize this, imagine the space trajectory being a circle in the horizontal plane and the time schedule specifying that the circle be followed at a given constant rate of speed. The pilot can accomplish this. The load factor and bank are determined by a universal relationship to rate and radius of turn. The pitch attitude is slaved to the angle of attack (AOA) that produces the requisite load at the given speed. The yaw input is, of course, slaved to the requirement of coordinated flight.

Orientation is defined by the space–time trajectory. The precise determination of pitch requires detailed knowledge of geometric and aerodynamic data of the particular airplane. On the other hand, the orientation of a system of "wind coordinates" aligned with the relative wind ("wind orientation") for the case of coordinated flight can be extracted from the trajectory by a universal algorithm that requires no data specific to the airplane type. This algorithm was given by one of us (AK) in a position paper to the sixth DIS workshop.[3] (The suggestion that some aircraft characteristics might be exploited in the extrapolation scheme has been voiced occasionally. The use of coordinated flight was mentioned at the 4th DIS workshop, but the algorithm for doing this was not given until the 6th workshop.)

The closed-form extraction algorithm obviates the necessity to extrapolate orientation variables. The difference between wind orientation and body orientation, for coordinated flight, is the AOA (Fig. 1). The AOA can be determined from the initial data and, if assumed constant, can subsequently be used to "correct" velocity orientation to body orientation. This is "extraction with correction" or EC, which we proposed for the first time in Ref. 4. We found the angle-of-attack correction crucial for the data we analyzed.

Extraction of the orientation can be applied together with any method for predicting the trajectory. We present results where it is used in conjunction with the assumption of constant Earth acceleration (CEA) in Sec. VIII.

While CEA is a useful common approach to extrapolating trajectory, it has long been felt that constant body accelerations are a better assumption where airplanes are concerned. We offer a variant of this concept in which the components of acceleration are constant in a velocity frame—a frame aligned with the velocity and the transverse acceleration. The result is a universal plane motion that admits closed-form expressions.[4] We refer to it as "constant longitudinal and transverse acceleration," or, in brief, CLTA. Extraction of orientation and CLTA are two independent algorithms. The former can be used with any method of trajectory extrapolation. The latter can be used with any method of orientation extrapolation. Put together as CLTA + EC, they make a complete closed-form extrapolation algorithm for airplanes.

CLTA may describe airplane flight better than CEA. This scheme will provide correct long-range predictions in a level turn. However, any pull-up or pushover would be continued

Received Feb. 14, 1994; revision received Oct. 1, 1994; accepted for publication Oct. 11, 1994.

*Professor, Department of Aerospace Engineering, P.O. Box 870280. Member AIAA.

†Graduate Student, Department of Aerospace Engineering, P.O. Box 870280. Student Member AIAA.

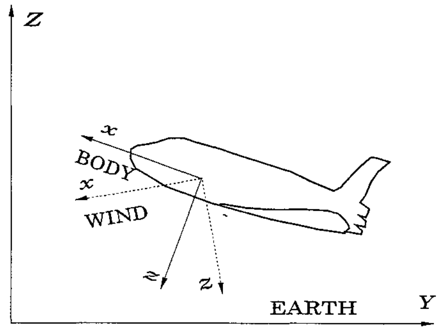

Fig. 1 Body and wind coordinates.

into an inside or an outside loop. This is avoided by our third algorithm—phugoid extrapolation.[4] The phugoid scheme offers a complete six degree-of-freedom extrapolation, with simplified airplane dynamics and coordinated flight built in. Left to its own devices, phugoid extrapolation will stabilize any mild transient condition into a stable level, climbing, or descending turn, or into a straight climb or descent, if initially unbanked.

The phugoid scheme assumes constant thrust, constant angle of attack, and coordinated flight. There are two modes of lateral control: 1) constant bank and 2) zero rate of roll. The first is appropriate for normal attitudes and maneuvers, the second to aerobatic flight. One mode or the other is selected based on attitude. The phugoid scheme, too, is based on the wind reference system, which can be propagated using universal relationships and requires a minimum of vehicle specific data. An AOA correction as described above is built in. The premise of constant AOA justifies using the AOA determined initially throughout the phugoid prediction.

The phugoid scheme is unable to predict what a pilot will do. It does predict what the airplane will do without conscious input from the pilot. Constant AOA roughly translates to heavy damping on any short period oscillation. Constant thrust roughly translates to constant throttle input. Constant bank and zero roll do require control inputs; however, these inputs are "psychomotor" as far as the pilot is concerned. Phugoid extrapolation requires an estimate of the aerodynamic efficiency (*L/D* ratio). It is not, however, overly sensitive to the estimate. Recall that *L/D* affects only the damping of phugoid oscillations and not their frequency.

Section III addresses trajectory geometry and kinematics. The scheme for extracting orientation from a given space–time trajectory is given in Sec. IV. Section V presents the closed-form expressions for trajectories maintaining constant longitudinal and transverse acceleration (CLTA). The phugoid scheme is defined in Sec. VI. Section VII describes exceptions to the various algorithms, which arise in special cases, and the work-arounds that we recommend. Section VIII presents the results of applying the airplane specific methods to sample data.

III. Trajectory Geometry and Kinematics

A space–time trajectory is a sequence of positions in three-space parameterized by time t. Geometrically, the space trajectory consists of the same sequence of positions, however parameterized. The natural geometric parameter is the arc length s. We denote derivatives with respect to s by a prime and derivatives with respect to t by a dot.

The basic geometric relationships are

$$\boldsymbol{r}' = \boldsymbol{e}_t \tag{1}$$

where $\boldsymbol{e}_t$ is a unit vector tangent to the trajectory:

$$\boldsymbol{r}'' = \boldsymbol{e}_t' = \kappa \boldsymbol{e}_n \tag{2}$$

Here, $\boldsymbol{e}_n$ is the unit vector along the first normal to the curve, and κ is the curvature, which is also the inverse of the local radius of the trajectory. A small segment of the trajectory can be approximated by a circular arc of radius $1/\kappa$ lying in the plane defined by $\boldsymbol{e}_t$ and $\boldsymbol{e}_n$. The second normal to the trajectory, which completes $\boldsymbol{e}_t$ and $\boldsymbol{e}_n$ to a right-handed triad is

$$\boldsymbol{e}_2 \equiv \boldsymbol{e}_t \times \boldsymbol{e}_n \tag{3}$$

Moving from geometry to kinematics, we now turn to the velocity $\boldsymbol{v}$, which is the time derivative of $\boldsymbol{r}$, and the acceleration $\boldsymbol{a}$, which is the second time derivative. In evaluating these we use Eqs. (1–3) and the chain rule of derivatives with

$$\dot{s} = v \tag{4}$$

We find

$$\boldsymbol{v} \equiv \dot{\boldsymbol{r}} = v\boldsymbol{e}_t \tag{5}$$

$$\boldsymbol{a} \equiv \dot{\boldsymbol{v}} = \dot{v}\boldsymbol{e}_t + \kappa v^2 \boldsymbol{e}_n \tag{6}$$

Thus, the velocity has the magnitude $\dot{s}$ and the direction of $\boldsymbol{e}_t$. The acceleration consists of a longitudinal component of magnitude $\dot{v}$ in the direction of $\boldsymbol{e}_t$, and a normal component (the centripetal acceleration) in the direction of the first normal $\boldsymbol{e}_n$.

Equations (5) and (6) may serve to define the longitudinal and normal acceleration, given the trajectory. In the alternative, when velocity and acceleration are given, the tangential direction is given by

$$\boldsymbol{e}_t = \boldsymbol{v}/v \tag{7}$$

The acceleration may be decomposed into a tangential component

$$\boldsymbol{a}_t = (\boldsymbol{a} \cdot \boldsymbol{e}_t)\boldsymbol{e}_t \tag{8}$$

and a normal component

$$\boldsymbol{a}_n = \boldsymbol{a} - \boldsymbol{a}_t \tag{9}$$

which is in the direction of the first normal.

IV. Extraction of Orientation from the Trajectory

We now get to the algorithm for extracting the airplane orientation from the trajectory. The orientation amounts to a definition of the body-fixed coordinate system in terms of an Earth-fixed system. To be definite, we adopt a body system with the x_b axis pointing forward towards the nose, the y_b axis pointing to the pilot's right towards the right wingtip, and the z_b axis directed down through the airplane's floor.

The extraction procedure actually addresses a different system of axes, known as "wind axis system." In this system, the x_w axis is aligned with the airplane's velocity vector. The body system is related to the wind system by a rotation in pitch equal to the airplane's AOA and a rotation in yaw equal to the sideslip angle. This last angle vanishes in coordinated flight. Assuming this, the y_w axis coincides with the y_b axis. The z_w axis completes the right-hand triad. The AOA can be determined from the initial data as the angle between x_b and $\boldsymbol{v}$. A correction by the AOA may be applied to the extracted wind orientation to estimate the true body orientation.

Denote the unit vectors in the x_w, y_w, and z_w directions, respectively, by $\boldsymbol{i}_w$, $\boldsymbol{j}_w$, and $\boldsymbol{k}_w$. We start by aligning the x_w axis with the trajectory

$$\boldsymbol{i}_w = \boldsymbol{e}_t \tag{10}$$

With this done, there still remains one degree of orientation freedom, namely, the rotation of the wind system around $\boldsymbol{e}_t$. This is done in the transverse plane, that is the plane orthogonal to $\boldsymbol{e}_t$. The acceleration $\boldsymbol{a}$ has already been decomposed into tangential and normal components in Eqs. (8) and (9). We similarly decompose the acceleration of gravity $\boldsymbol{g}$ into a longitudinal component

$$\boldsymbol{g}_t = (\boldsymbol{g}\cdot\boldsymbol{e}_t)\boldsymbol{e}_t \tag{11}$$

and a normal component

$$\boldsymbol{g}_n = \boldsymbol{g} - \boldsymbol{g}_t \tag{12}$$

The balance of normal specific forces is expressed by

$$\boldsymbol{l} = \boldsymbol{a}_n - \boldsymbol{g}_n \tag{13}$$

where $\boldsymbol{l}$ is the active normal specific force; in airplane terms this is the lift divided by the mass. The vectors on the right side of Eq. (13) are defined in Eqs. (9) and (12). Equation (13) in turn determines $\boldsymbol{l}$.

The condition of coordinated flight is that $\boldsymbol{l}$ be in the direction of the negative z_w axis:

$$\boldsymbol{k}_w = -(\boldsymbol{l}/l) \tag{14}$$

The body triad is completed by

$$\boldsymbol{j}_w = \boldsymbol{k}_w \times \boldsymbol{i}_w \tag{15}$$

When the vectors $\boldsymbol{i}_w, \boldsymbol{j}_w, \boldsymbol{k}_w$ are expressed in an Earth coordinate system X, Y, Z, the matrix of components

$$M_w = \begin{bmatrix} i_{wX} & j_{wX} & k_{wX} \\ i_{wY} & j_{wY} & k_{wY} \\ i_{wZ} & j_{wZ} & k_{wZ} \end{bmatrix} \tag{16}$$

describes the active rotation from Earth to wind coordinates.

If the AOA correction is to be employed, the correction may be computed once from the initial data and applied every time the orientation is used for visual presentation. For illustration, assume that orientation is expressed as a rotation matrix M (the active rotation from Earth coordinates). From the initial body orientation M_b and the initial M_w of Eq. (16), compute the correction matrix:

$$M_{\mathrm{cor}} = M_w^T M_b \tag{17}$$

Then, once the extrapolated M_w is obtained, M_b may be produced as

$$M_b = M_w M_{\mathrm{cor}} \tag{18}$$

An analogous procedure applies to quaternions. Euler angles may be converted to one or the other.

V. Trajectory Extrapolation

There still remains the question of extrapolating the trajectory. In this section this is addressed based on the assumption of components of acceleration being constant in velocity coordinates. Closed-form results are derived.

It is common practice to extrapolate based on a constant value of Earth acceleration. This amounts to fitting a parabola in the plane of $\boldsymbol{e}_t$ and $\boldsymbol{e}_n$ to represent the trajectory. There aren't many flight maneuvers that maintain constant (nonzero) Earth acceleration. Keeping the body components of acceleration constant may have a slightly wider applicability. Use of actual body orientation requires knowledge of details of the configuration of the particular airplane. But use of a velocity frame aligned with $\boldsymbol{e}_t$, $\boldsymbol{e}_n$, and $\boldsymbol{e}_2$ of Eqs. (1–3) supports universal relationships.

Assuming that the tangential and normal components of acceleration in Eq. (6) are both constants, which we denote A and B respectively, we find

$$\dot{v} = A \tag{19}$$

$$\kappa v^2 = B \tag{20}$$

Equation (19) integrates into

$$v = v_0 + At \tag{21}$$

We further suppose that the motion stays in the plane defined by the initial $\boldsymbol{e}_t$ and $\boldsymbol{e}_n$. Multiply Eq. (2) by $\dot{s} = v$ to find

$$\dot{\boldsymbol{e}}_t = v\kappa\boldsymbol{e}_n \tag{22}$$

This identifies the angular velocity of $\boldsymbol{e}_t$ and $\boldsymbol{e}_n$ in their plane as

$$\dot{\theta} = v\kappa \tag{23}$$

where θ is the angle of $\boldsymbol{e}_t$ with an Earth-fixed x_p axis in the plane of the motion. Now use Eqs. (20) and (21) to recast Eq. (23) as

$$\dot{\theta} = B/v = B/(v_0 + At) \tag{24}$$

The last equation integrates into

$$\theta = (B/A)\ell n|1 + (At/v_0)| = (B/A)\ell n|v/v_0| \tag{25}$$

To complete the integration of the trajectory we must determine the position of the airplane. We do this first in a system of coordinates x_p, y_p in the plane of the motion with the x_p axis along the initial $\boldsymbol{e}_t$ and the y_p axis along the initial $\boldsymbol{e}_n$ (see Fig. 2). The governing differential equations are

$$\dot{x}_p = v\cos\theta \tag{26}$$

$$\dot{y}_p = v\sin\theta \tag{27}$$

To proceed from here, divide the last two equations by Eq. (24) to obtain

$$\frac{\mathrm{d}x_p}{\mathrm{d}\theta} = \frac{v^2}{B}\cos\theta \tag{28}$$

$$\frac{\mathrm{d}y_p}{\mathrm{d}\theta} = \frac{v^2}{B}\sin\theta \tag{29}$$

Now rearrange Eq. (25) as

$$v = \pm v_0 e^{(A/B)\theta} \tag{30}$$

and substitute into Eqs. (28) and (29). The result is

$$\frac{\mathrm{d}x_p}{\mathrm{d}\theta} = \frac{v_0^2}{B}e^{2(A/B)\theta}\cos\theta \tag{31}$$

$$\frac{\mathrm{d}y_p}{\mathrm{d}\theta} = \frac{v_0^2}{B}e^{2(A/B)\theta}\sin\theta \tag{32}$$

The last two equations are reduced by quadrature to

$$x_p = \frac{v_0^2}{4A^2 + B^2}e^{2(A/B)\theta}(2A\cos\theta + B\sin\theta) \tag{33}$$

$$y_p = \frac{v_0^2}{4A^2 + B^2}e^{2(A/B)\theta}(2A\sin\theta - B\cos\theta) \tag{34}$$

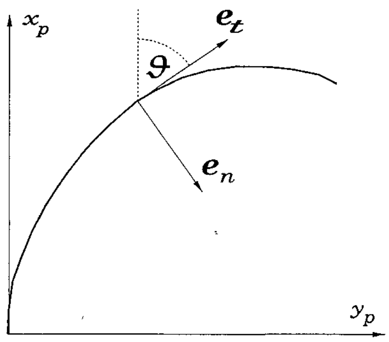

Fig. 2 CLTA plane.

Equations (33) and (34) describe a family of curves that depend on only two parameters, which may be selected as

$$\alpha \equiv A/B \tag{35}$$

$$c \equiv Bv_0^2/(4A^2 + B^2) \tag{36}$$

In terms of these, Eqs. (33) and (34) can be rewritten as

$$x_p = ce^{2\alpha\theta}(2\alpha \cos \theta + \sin \theta) \tag{37}$$

$$y_p = ce^{2\alpha\theta}(2\alpha \sin \theta - \cos \theta) \tag{38}$$

where c has a dimension of length and serves as a scale factor for the trajectory. α is dimensionless and determines its shape. Each trajectory is a spiral that converges to the origin on one side and spreads out to infinity on the other. Figure 3, a plot of y_p/c against x_p/c, is a sample curve for $\alpha = 0.125$.

Each spiral is self-similar, and any two points on the spiral are equivalent in the following sense: any selected point on the spiral may be moved to any other selected point by a similarity transformation, consisting of rotation and dilation, that maps the spiral onto itself.

The velocity vector $\boldsymbol{v}$ and the position vector $\boldsymbol{r}$ relative to the Earth system origin are given by

$$\boldsymbol{v} = v(\cos \theta\, \boldsymbol{e}_{t0} + \sin \theta\, \boldsymbol{e}_{n0}) \tag{39}$$

$$\boldsymbol{r} = \boldsymbol{r}_0 + (x_p - 2\alpha c)\boldsymbol{e}_{t0} + (y_p + c)\boldsymbol{e}_{n0} \tag{40}$$

where $\boldsymbol{e}_{t0}$ and $\boldsymbol{e}_{n0}$ are the unit vectors in the initial tangential and normal directions, respectively. The full closed form procedure is as follows:

1) Determine the initial parameters $\boldsymbol{e}_{t0}$, $\boldsymbol{e}_{n0}$, v_0, θ_0, A, and B from the initial data.
2) Compute c and α [Eqs. (35) and (36)].
3) Compute v in terms of t [Eq. (21)].
4) Calculate θ in terms of v [Eq. (25)].
5) Find x_p, y_p in terms of θ [Eqs. (37) and (38)].
6) Obtain $\boldsymbol{v}$ and $\boldsymbol{r}$ [Eqs. (39) and (40)].

The derivations above assume that $A \neq 0$ and $B \neq 0$. Should B vanish, then, from Eq. (24) θ is a constant, the velocity frame does not rotate, and its motion is rectilinear. The equations for constant acceleration in Earth coordinates apply. (The case that both A and B vanish is included.) If $A = 0$, but $B \neq 0$, the trajectory is a circle in the plane containing the velocity vector and the acceleration vector. The speed and the angular velocity of $\boldsymbol{e}_t$ and $\boldsymbol{e}_n$ in their plane remain constant. The angle θ becomes

$$\theta = (B/v)t \tag{41}$$

Equations (33) and (34) reduce to

$$x_p = (v^2/B)\sin \theta \tag{42}$$

$$y_p = -(v^2/B)\cos \theta \tag{43}$$

which describe a circle with its center at $x_p = 0$, $y_p = 0$.

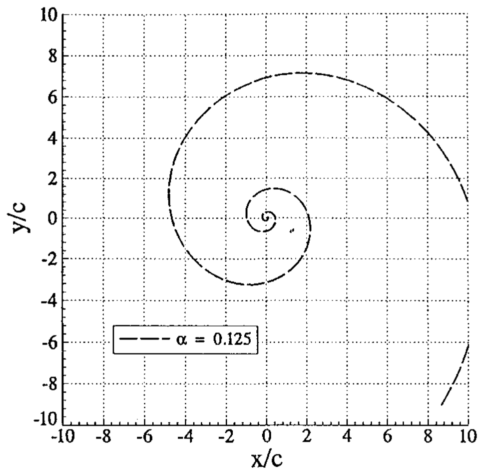

Fig. 3 CLTA trajectory.

The breaking of the initial acceleration into a tangential component A and a normal component B is ill-defined when the velocity vanishes. However, the velocity that immediately builds up is in the direction of the acceleration. For this reason we interpret all the acceleration in this case as being tangential

$$A = a \qquad B = 0 \tag{44}$$

A more rigorous explanation of this point is as follows: Decompose the acceleration at a slightly later time δt into longitudinal and transverse components, and take the limit $\delta t \to 0$. By a well-known theorem of calculus about the limit of a quotient with both numerator and denominator vanishing:

$$\lim A = \lim(\boldsymbol{a} \cdot \boldsymbol{v})/v = \lim(\boldsymbol{a} \cdot \boldsymbol{a})/a = a \tag{45}$$

Similarly

$$\lim B = \lim\sqrt{a^2 - A^2} = 0 \tag{46}$$

VI. Phugoid Extrapolation Scheme

Both of the schemes of the previous section ignore some of the facts of life of ordinary flying: That the acceleration of gravity $\boldsymbol{g}$ is significant compared to specific forces created by an airplane; that a tangential component of $\boldsymbol{g}$ will cause significant changes in speed; that speed is a necessary ingredient in generating normal loads. All of these observations are reflected in the phugoid extrapolation scheme introduced in this section.

We assume that the four DOF at the disposal of the pilot are used to maintain 1) constant angle of attack, 2) constant thrust, 3) constant bank (mode a) or zero rate of roll (mode b), and 4) coordinated flight (zero sideslip angle).

Assumption 1 translates into both lift and drag being proportional to v^2 with constant coefficients. Using the decomposition of $\boldsymbol{a}$ and $\boldsymbol{g}$ into tangential and normal components [Eqs. (8), (9), and (11–13)] we postulate

$$\boldsymbol{l} = -\boldsymbol{k}Pv^2 \tag{47}$$

$$a_t - g_t = Q - Rv^2 \tag{48}$$

where P, Q, R are constant. Note that P is positive by the definition of $\boldsymbol{k}$ [Eq. (14)]; R is positive because of the nature of drag; Q is positive so long as the thrust is in the direction of flight.

The bank of the wind frame is the angle between the k_w axis and $\boldsymbol{g}_n$. This angle is determined from the initial $\boldsymbol{l}$ and $\boldsymbol{g}_n$ and, in mode a, maintained constant.

The constant P can be determined from the initial values of the variables in Eq. (47). However, Eq. (48) is insufficient to determine Q and R individually. To overcome this, a value of aerodynamic efficiency

$$\eta = \text{lift/drag} = P/R \tag{49}$$

must be obtained or assumed. Armed with a value of η, Eq. (48) may be restated as

$$a_t - g_t = Q - (P/\eta)v^2 \tag{50}$$

With P determined by the initial value of Eq. (47), Q may be obtained from the initial values in Eq. (50). Armed with these constants, we can now determine the trajectory for all time.

The governing differential equations are

$$\dot{\boldsymbol{r}} = v\boldsymbol{e}_t \tag{51}$$

$$\dot{v} = Q - (P/\eta)v^2 + g_t \tag{52}$$

$$\dot{\boldsymbol{e}}_t = -Pv\boldsymbol{k} + \boldsymbol{g}_n/v \tag{53}$$

We also have

$$\dot{\boldsymbol{e}}_t = \boldsymbol{\omega} \times \boldsymbol{e}_t \tag{54}$$

Now express $\boldsymbol{\omega}$ and $\boldsymbol{g}$ in component form as

$$\boldsymbol{\omega} = \omega_1\boldsymbol{i} + \omega_2\boldsymbol{j} + \omega_3\boldsymbol{k} \tag{55}$$

$$\boldsymbol{g} = g_1\boldsymbol{i} + g_2\boldsymbol{j} + g_3\boldsymbol{k} \tag{56}$$

We equate Eq. (53) to Eq. (54), and substitute the appropriate components of Eqs. (55) and (56), to obtain

$$-\omega_2\boldsymbol{k} + \omega_3\boldsymbol{j} = -Pv\boldsymbol{k} + (g_2\boldsymbol{j} + g_3\boldsymbol{k})/v \tag{57}$$

which yields

$$\omega_2 = Pv - g_3/v \tag{58}$$

$$\omega_3 = g_2/v \tag{59}$$

Maintaining these values for ω_2 and ω_3 enforces the condition of coordinated flight. However, the roll rate ω_1 is still unspecified.

In mode a, the roll rate is determined by the condition of constant bank. Maintaining the angle between $\boldsymbol{k}$ and g_n requires that the ratio of the components of $\boldsymbol{g}_n$ (g_2 and g_3) remain constant. This is expressed as

$$\frac{\mathrm{d}}{\mathrm{d}t}\left(\frac{g_2}{g_3}\right) = \frac{\dot{g}_2}{g_3} - \frac{g_2\dot{g}_3}{g_3^2} = 0 \tag{60}$$

From

$$\dot{\boldsymbol{g}} = \boldsymbol{\omega} \times \boldsymbol{g} \tag{61}$$

we obtain

$$\dot{g}_2 = \omega_3 g_1 - \omega_1 g_3 \tag{62}$$

$$\dot{g}_3 = \omega_1 g_2 - \omega_2 g_1 \tag{63}$$

Substituting Eqs. (62) and (63) into Eq. (60) and solving for the roll rate, we find

$$\omega_1 = g_1 \frac{\omega_2 g_2 + \omega_3 g_3}{g_2^2 + g_3^2} \qquad \text{(mode a)} \tag{64}$$

In mode b, Eq. (64) is replaced by

$$\omega_1 = 0 \qquad \text{(mode b)} \tag{65}$$

With the above equations for the rotational rates and accelerations, the position of the airplane and its velocity system orientation are defined for all time. They can be computed by numerical integration.

The selection of the mode used for determining the roll rate, mode a or mode b, is based on the attitude. So long as both pitch and bank stay within predetermined thresholds, mode a is used. Should one of the thresholds be exceeded, mode b is selected. Mode a stabilizes pull-ups and pushovers into gentle climbing or descending spirals or straight flight paths. This is representative of ordinary flying and transport-type maneuvers. Mode b is suitable for acrobatic flying, and will easily describe vertical and oblique loops. Mode a, if maintained with the pitch attitude approaching the vertical, results in rapid rolling. The rate of roll diverges as the pitch attitude becomes 90 deg up or 90 deg down. However, long before a condition like this is reached, we will have switched to mode b.

It must be stressed that the procedure so far described extrapolates wind orientation. It is still necessary to apply an AOA correction. This is done as described in Sec. III. In the case of the phugoid scheme, the use of a constant AOA correction is fully justified, since the AOA is kept constant.

The phugoid scheme requires an estimate of η, the aerodynamic efficiency. The accuracy of this parameter is not crucial. It determines the damping of the phugoid motion. The frequency is independent of it. In the evaluation of Sec. VIII we set it arbitrarily to 10.

VII. Exceptions

The equations presented above for extraction of the orientation and for extrapolation of the trajectory are valid for most flight conditions. However, there are a few discrete conditions for which the equations fail. These conditions, and the methods that were employed to work around the singularities they cause, are described in this section.

The procedure for extracting the orientation from the trajectory (Sec. III) becomes undefined under two conditions:

1) The method aligns the x_w axis with the velocity vector. This cannot be done when the aircraft translational velocity is zero. For this case, we fall back on the method of constant angular velocity, and determine the new orientation from the previous orientation, based on the rotational rate and the elapsed time.

2) The method also fails when the active normal specific force $\boldsymbol{l}$ vanishes (flight at "zero g"). In this situation, the bank cannot be determined. Instead, the aircraft is assumed to achieve its new orientation by the smallest rotation that aligns the x_w axis correctly.

This is a rotation about an axis that is perpendicular to both the original x_w axis and the new x_w axis.

The phugoid scheme depends on resolving quantities such as the acceleration of the airplane and the acceleration of gravity into longitudinal and transverse components. This cannot be done when the velocity vanishes. For this reason, when the velocity is below a predetermined limit, we fall back to either of the orientation extrapolation schemes described above and to trajectory extrapolation using CEA.

Note that a traditional airplane cannot achieve zero speed except momentarily at the point of a tail slide. At that point the airplane undergoes a violent change of orientation. No harm would result if the phugoid approximation adopted a "do nothing" rule in the case of vanishing velocity, so long as it is applied to an airplane. The reason for falling back on the more traditional approach at extremely low speed is to try to accommodate other vehicles, e.g., helicopters.

VIII. Evaluation

The algorithms of the previous sections were coded as *C* subroutines and embedded in a program that exercised them for evaluation against recorded flight histories.

Table 1 shows comparative figures of merit for different methods of extrapolation. The table lists the number of updates that were generated when the dead reckoning error exceeded a position threshold of 10 ft or an orientation threshold of 10 deg. Coordinate invariant thresholds are used. The position threshold applies to the distance between the predicted position and the true position. The orientation threshold applies to the angle of the short rotation between the predicted orientation and true orientation. In this way the history of updates is independent of the choice of coordinates and of the heading on which a maneuver is started. Invariant tolerances result in more updates than the same thresholds values, applied to individual coordinates or to individual Euler angles, as is done in Refs. 2 and 5.

The different extrapolation techniques are applied in Table 1 to the same flight history of an F-16. The flight sequence was generated at Luke Air Force Base. It is illustrated in Fig. 4. (See Ref. 5 for additional analysis of the same data.) The airplane maneuvered mainly in the vertical plane, going through two consecutive loops. The history covers 35 s of flight. The AOA was high throughout, exceeding 20 deg, which made AOA correction very important. Both orientation extraction and the phugoid performed very well.

Table 1 is arranged as a matrix. The columns contain results obtained with different methods of orientation prediction with the method of trajectory extrapolation remaining the same. This is reversed with the rows. The phugoid method, which cannot be mixed, results in a few entries of "NA." Perfect orientation (last row) and perfect trajectory (last column) are included for comparison.

Inspection of Table 1 shows that the use of extraction with correction (EC) for predicting orientation more than halved the number of required updates as compared with constant angular rates (CAR), the method of extrapolating the trajectory being the same. What is more, the results employing EC are very close to comparison data using the true orientation. In other words, coupled with either CEA or CLTA, EC is nearly perfect. The table shows only modest improvement when CLTA is substituted for CEA, with the method of predicting orientation remaining the same.

The pre-existing combination of CEA and CAR (CEA + CAR) was doing well in requiring only 81 updates for the 1409 frame history. The all new combination of CLTA + EC reduced this further to only 30 (a factor of 2.7). The phugoid scheme did even slightly better, requiring only 27 updates (improvement by a factor of 3).

Table 1 Performance comparison using F-16 data

	CEA	CLTA	Phugoid	True trajectory
CAR	81	78	NA	75
EC	36	30	NA	22
Phugoid	NA	NA	27	NA
True orientation	33	28	NA	0

Number of updates in 1409 frames to maintain a tolerance of 10 ft and 10 deg.

Table 2 offers data obtained with additional flight trajectories. Only the extrapolation methods corresponding to the diagonal positions in Table 1 are represented. Since the duration of the various flight histories are not equal, the data is stated in terms of updates per second. The F-16 data of Table 1 is included for comparison.

The histories include two sequences of X-31 maneuvering flight generated at NASA Dryden; a UH-1 helicopter in translational flight flown by an Army aviator at the University of Alabama Flight Dynamics Lab; and an F-16 wingman flying formation with the first F-16 generated from the original F-16 data. The wingman was postulated to maintain a rigid side-by-side formation with his wingtip separated laterally from the leader's wingtip by 10 ft.

The X-31 data was taken with thrust vectoring disabled. Thrust vectoring would severely violate the assumptions made in deriving the new extrapolation methods. Even so, we distinguish one sequence that was uncoordinated to the extent of almost 0.5 *g* of lateral load from another that was basically coordinated with side loads limited to less than 0.1 *g*. The wingman and the helicopter are also uncoordinated. The wingman is forced to deviate from coordinated flight to maintain the rigid formation. The helicopter deviates from airplane style coordinated flight because of the side force generated by its tail rotor.

All cases show gains for the airplane specific methods. Surprisingly, there are gains, albeit more modest, even for the histories where the assumption of coordinated flight is not strictly satisfied. An exhaustive study of the relative merit of the new methods for all aircraft and all flight regimes is outside the scope of this article. However, Table 2 serves to illustrate that significant gains are not exceptional.

Even though developed with distributed simulation in mind, the methods presented here may be of value in other applications. Ground-to-air and air-to-air weaponry could be one instance.

The approach of exploiting knowledge specific to the category of vehicle could be extended to helicopters, ground

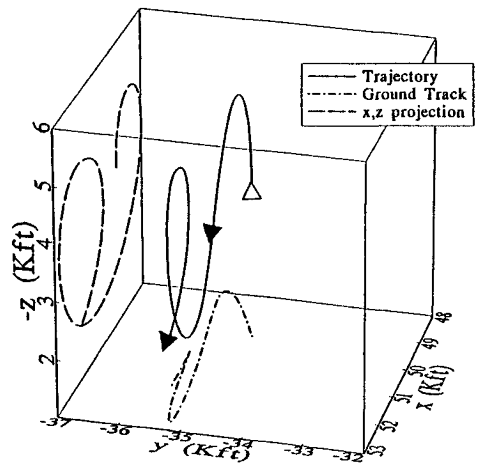

Fig. 4 F-16 flight trajectory.

Table 2 Additional performance comparisons

	CEA + CAR	CLTA + EC	Phugoid	Improvement factor
F-16	2.23	0.85	0.77	3.0
F-16 wingman	3.24	1.90	1.96	1.7
X-31	1.63	0.43	0.33	4.9
X-31 uncoordinated	1.13	0.86	0.76	1.5
UH-1	0.780	0.427	0.416	1.9

Number of updates per second to maintain a tolerance of 10 ft and 10 deg.

vehicles, supersonic aircraft and missiles, and ballistic missiles.

Acknowledgments

The work reported here was supported by Loral Western Development Labs under Subcontract SO-242825-A. We are indebted to Kurt Lin of UCF IST for providing F-16 flight data, and to Larry Schilling and Ken Norlin of NASA Dryden for the X-31 data. The UH-1 data was obtained in our own lab with Captain Mark Jackson of the U.S. Army flying the simulator. Jerry Vanpelt helped proof the manuscript.

References

[1]*IEEE Standard for Information Technology—Protocols for Distributed Interactive Simulation Applications*, Inst. of Electrical and Electronics Engineers, IEEE Std. 1278-1993, New York, 1993.

[2]Goel, S., and Morris, K., "Dead Reckoning for Aircraft in Distributed Interactive Simulation," *AIAA Flight Simulation Technologies Conference* (Hilton Head, SC), AIAA, Washington, DC, 1992, p. 277.

[3]Katz, A., "Notes on Dead Reckoning in the DIS Standard," *Position Paper, Sixth Workshop on Distributive Interactive Simulation* (Orlando, FL), Vol. II, Inst. for Simulation and Training, Univ. of Central Florida, Orlando, FL, 1992, p. 115.

[4]Katz, A., and Graham, K., "Extrapolation of Airplane Flight," Loral Western Development Labs, UA FDL Rept. 93S03, under Subcontract SO-242825-A, Item 04, San Jose, CA, Dec. 17, 1993.

[5]Lin, K. C., and Schab, D. E., "Study on the Network Load in Distributed Interactive Simulation," *AIAA Flight Simulation Technologies Conference* (Scottsdale, AZ), AIAA, Washington, DC, 1994, pp. 202–209.